Uncertainty in Steady-State Diagnostics of a Current-Pressure Transducer: How Confident are We in Diagnosing Faults?

Shankar Sankararaman[1], Christopher Teubert[2], and Kai Goebel[3]

[1,2] *SGT Inc., NASA Ames Research Center, Moffett Field, CA 94035, USA*
shankar.sankararaman@nasa.gov
christopher.a.teubert@nasa.gov

[3] *NASA Ames Research Center, Moffett Field, CA 94035, USA*
kai.goebel@nasa.gov

ABSTRACT

Current-Pressure (I/P) transducers are effective pressure regulators that can vary the output pressure depending on the supplied electrical current signal, and are commonly used in pneumatic actuators and valves. Faults in current-pressure transducers have a significant impact on the regulation mechanism, and therefore, it is important to perform diagnosis to identify such faults. However, there are different sources of uncertainty that significantly affect the diagnostics procedure, and therefore, it may not be possible to perform fault diagnosis and prognosis accurately, with complete confidence. These sources of uncertainty include natural variability, sensor errors (gain, bias, noise), model uncertainty, etc. This paper presents a computational methodology to quantify the uncertainty and thereby estimate the confidence in the fault diagnosis of a current-pressure transducer. First, experiments are conducted to study the nominal and off-nominal behavior of the I/P transducer; however, sensor measurements are not fast enough to capture brief transient states that are indicative of wear, and hence, steady-state measurements are directly used for fault diagnosis. Second, the results of these experiments are used to train a Gaussian process model using machine learning principles. Finally, a Bayesian inference methodology is developed to quantify the uncertainty and assess the confidence in fault diagnosis by systematically accounting for the aforementioned sources of uncertainty.

1. INTRODUCTION

Current-Pressure transducers (I/P transducer or IPT) are effective pressure regulators that vary the output pressure depending on the supplied electrical current signal. They operate by throttling a nozzle to create a pressure difference across a diaphragm, which, in turn, controls the throttling of a valve. These are often used for supplying precise pressures to control pneumatic actuators and valves. When such transducers are subjected to wear, it may not be possible to efficiently regulate currents so that desired output pressures may be generated. Therefore, it is necessary to constantly monitor the performance of the transducer using efficient health management techniques and continuously perform diagnosis and prognosis, i.e., detect, isolate, and estimate faults and quantify the remaining useful life of the transducer. Wear detection, estimation, and prediction play a critical role in preventing failure, scheduling maintenance, and improving system utility.

An important challenge in health management is the presence of several sources of uncertainty that affect both diagnosis and prognosis. These sources of uncertainty are present in measurement sensors, system models, and the system inputs. Due to these sources of uncertainty, it becomes necessary to quantify the confidence in the results of diagnosis and prognosis. This can be addressed by estimating the uncertainty in the results of diagnosis (Sankararaman & Mahadevan, 2011, 2013) by rigorously accounting for these sources of uncertainty during health monitoring. While these preliminary methods for uncertainty quantification in diagnosis have been developed from a statistical point of view, it is still necessary to explore the applicability of these methods to different types of practical applications where the impact of uncertainty is extremely significant. While the above statistical methods can efficiently diagnose abrupt faults, wear in practical applications is usually continuous and hence, more challenging from the point of diagnosis and uncertainty quantification.

This paper focuses on applying uncertainty quantification methods to continuous wear estimation in the aforementioned current-pressure transducer. Previous studies at NASA Ames Research Center (Teubert & Daigle, 2013) have ob-

served that there is a significant amount of uncertainty during the health monitoring of the aforementioned current-pressure transducer; however, the effects of uncertainty on the IPT steady-state diagnosis and prognosis were not studied because simplistic look-up tables had been used for fault estimation. In order to apply rigorous uncertainty quantification methods, it is first necessary to identify and address certain application-specific challenges. In the case of the current-pressure transducer, the challenge lies in obtaining useful information from the sensors used in the health monitoring system. To begin with, there is a significant amount of noise and uncertainty in the sensor measurements. More importantly, the sensors are not fast enough to capture brief transient states; this can either be a result of sensor technological limits, or budgetary constraints on sensor selection (as sensors with higher resolution and higher sampling frequencies are generally more expensive). Many modern wear estimation diagnostic techniques rely on the measurement of the system's transient states (Daigle & Goebel, 2013; Orchard & Vachtsevanos, 2009; Saha & Goebel, 2009; Luo, Pattipati, Qiao, & Chigusa, 2008), and therefore, these techniques cannot be used for diagnosis of the current-pressure transducer. In order to overcome this challenge, researchers at NASA Ames Research Center (Teubert & Daigle, 2013) are pursuing a diagnostic methodology that relies only on steady-state measurements without using any transient information. Therefore, it is necessary to rely on such steady-steady measurements while quantifying the uncertainty in diagnosis.

The primary goal of this paper is to develop a computational methodology to assess the impact of the different sources of uncertainty on wear estimation in the current-pressure transducer, and in turn, quantify the uncertainty in diagnostics. First, experimental data are collected to study the relationship between the input currents, fault magnitudes, and the output pressures, and the resulting data are used to develop a Gaussian process model that can predict the output pressures as a function of input currents and fault magnitude. This model is built offline using principles of machine learning, and then used for diagnosis during online health monitoring. A Bayesian inference-based methodology is developed to quantify the extent of wear, and the associated uncertainty. This analysis is continuously performed in order to continuously estimate the wear and thereby, the fault magnitude can be quantified as a function of time. The Bayesian inference-based methodology provides a systematic framework for including different sources of uncertainty and quantifying the combined effect of the different sources of uncertainty on fault estimation uncertainty, thus providing an estimate in the confidence in diagnosis.

The paper is organized as follows. Section 2 describes the current-pressure transducer in detail, and explains the various modeling and experimental aspects of the transducer. Section 3 describes the Gaussian process modeling methodology

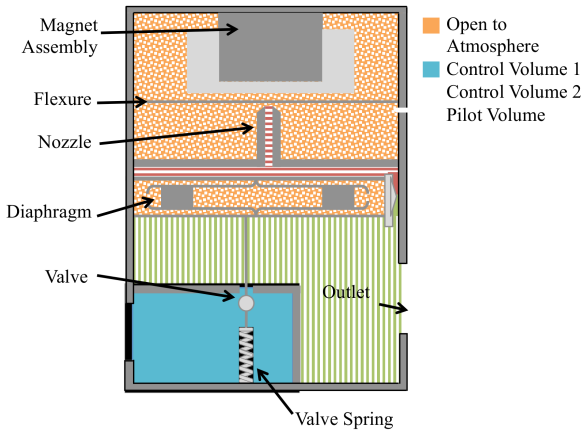

Figure 1. Current/pressure transducer schematic.

Figure 2. Current/pressure transducer.

that is used as a machine learning tool to model the nominal and off-nominal behavior of the current-pressure transducer, and in turn used for diagnosis. Section 4 describes the Bayesian inference-based methodology for quantifying the uncertainty in diagnosis, using the aforementioned Gaussian process model. A simplistic metric for confidence assessment in diagnostics is also presented. Finally, the numerical results are described in Section 5, and conclusions are presented in Section 6.

2. DESCRIPTION OF THE TRANSDUCER

This section describes the behavior of the current-pressure transducer in detail, by exploring both nominal and off-nomoinal (faulty) conditions. Consider a Marsh Bellofram Type 1000 IPT, as shown in Figures 1 and 2. Some specifications for this IPT are included in Table 1 (Marsh Bellofram, n.d.). This particular transducer was chosen because of its use for cryogenic propellant loading applications, and, specifically in the Prognostics Demonstration Testbed at NASA Ames Research Center (Kulkarni, Daigle, & Goebel, 2013).

The IPT is divided into three distinct control volumes (CVs): Control Volume 1 (CV1) at the inlet, Control Volume 2 (CV2)

Table 1. IPT specifications

Name	Type 1000 IPT
Manufacturer	Marsh Bellofram
Supply Pressure Range	18-100 psig
Input Signal Range	4-20 mA
Output Pressure Range	3-15 psig

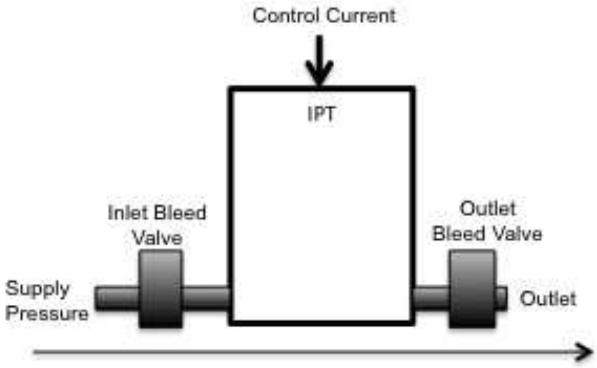

Figure 3. IPT testing configuration

at the outlet, and the Pilot Control Volume (CVP) at the nozzle. Each control volume is marked in a different color and pattern in Figure 1. The IPT output pressure varies with the current supplied to the magnet assembly. When the current is high, the magnet assembly throttles the flow out of the pilot nozzle, allowing less air to escape through the nozzle. With a low input current, more gas escapes from the nozzle thereby lowering the pilot pressure. The pressure difference across the diaphragm moves the valve, which adjusts the gas flow between CV1 and CV2. Adjusting this flow changes the pressure in CV2, and thus provides a direct mechanism to regulate the outlet pressure. In past research efforts, the behavior of this transducer has been modeled using a physics-based approach (Teubert & Daigle, 2013, 2014); however, this model is not used in this paper. Instead, a completely data-driven approach is used for both performance prediction and health monitoring. The experimental set-up for generating data is described in the next subsection.

2.1. Experimental setup

In order to study the nominal and faulty performance of the transducer, a series of experiments were conducted using the Prognostics Demonstration Testbed at NASA Ames Research Center. The Prognostics Demonstration Testbed (Kulkarni et al., 2013) was developed to demonstrate cryogenic refueling valve prognosis. This testbed included an I/P Transducer that was used to operate a large valve. The section of the testbed including the I/P Transducer is illustrated in Figure 3.

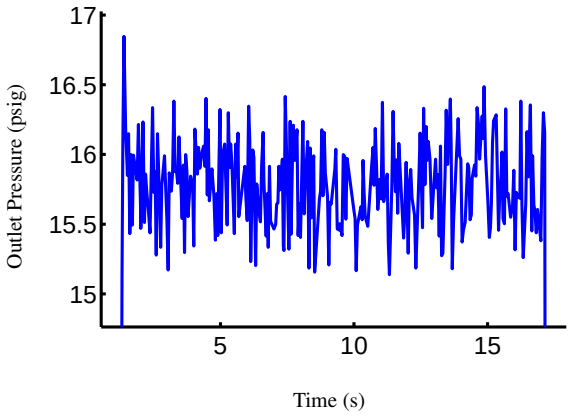

Figure 4. IPT outlet pressure with time

As seen in the figure, two bleed valves were installed on the IPT line: one upstream, and one downstream. These valves were used to simulate inlet and outlet leaks, respectively. A pressure of 75 psig is supplied using a pump. Data were collected from pressure sensors located before the inlet bleed valve and after the outlet bleed valve at a frequency of 16.8 Hz using an 8-slot NI cDAQ-9188 Gigabit Ethernet chassis data acquisition (DAQ) system (Kulkarni et al., 2013). A control input is supplied to the IPT. A separate control input is supplied to the bleed valves to create a leak.

2.2. Nominal IPT Behavior

The IPT documentation indicated the IPT should produce an outlet pressure of 3 and 20 psig when supplied a signal current of 4 and 20 mA, respectively (Marsh Bellofram, n.d.). In this range, the pressure changes linearly with input current.

In practice, IPT behavior is much more difficult to understand. Noise as much as 10% was observed in measurements of outlet pressure, as seen in the experimental data included in Figure 4. This figure shows the measured outlet pressure with time. This noise complicates the process of measuring the steady-state pressure, and thereby complicates the diagnosis procedure. Hence, a rigorous diagnosis methodology should be able to separate the effect of the noise; in fact, this is a prominent feature of the diagnosis method proposed in this paper (in Section 4).

Additionally, it was observed that the pressure at a given input current would vary from day to day but was generally constant over the course of one experiment. We will henceforth refer to this phenomena as "wandering set-point". A histogram showing the spread of steady state pressure measurements over 676 cycles with an input current of $4mA$ is included in Figure 5. In this figure, the input current predicted by the model and documentation is indicated by a dashed red line.

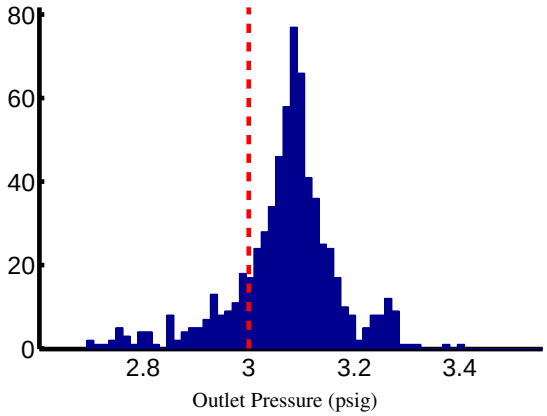

Figure 5. Histogram of IPT steady-state outlet pressure for an input current of 4 mA

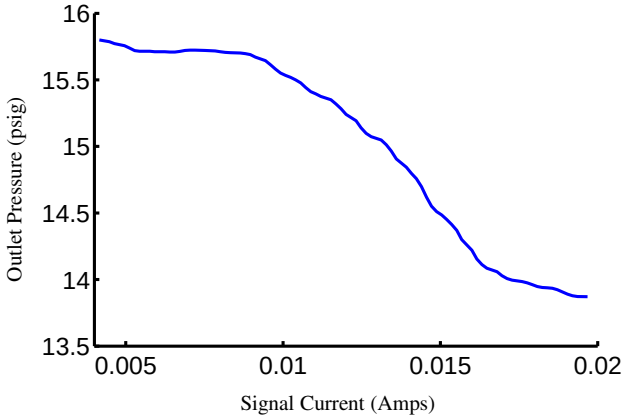

Figure 6. Outlet leak

An experiment was conducted to determine if wandering set-point is observable over the course of one experiment. These experiments found that after 200 minutes of consistent operation there was no observable wandering set-point. From this it was concluded that this phenomena will not occur during the course of a single experiment. In this paper, the wandering set-points are directly included into the data-driven modeling framework, and accounted for during diagnosis, as explained in Sections 4 and 5.

2.3. IPT Wear

Through discussions with the manufacturers and with users of I/P transducers and similar components four possible wear modes were indicated. These wear modes are described below:

1. **Leaks** A leak could occur at the inlet (inlet leak), at the outlet (outlet leak), at the valve (valve seat leak), or at the nozzle (pilot leak).
2. **Spring Weakening** A weakening of the valve spring, the diaphragm, or the flexure. This will decrease the spring coefficient of the effected system.
3. **Valve Impediment** A impediment or "clog" at the valve opening between $CV1$ and $CV2$. This can be caused by foreign object contamination.
4. **Magnet Assembly Weakening** A weakening of the magnet assembly with use.

Though all these faults are possible, this paper focuses only on outlet leak faults. Outlet leaks were chosen because they are well understood and can be directly simulated while performing experiments. Only this fault and inlet leaks can be simulated in the laboratory with our current experimental setup. Studies show that introducing an inlet leak has very little effect on IPT performance (Teubert & Daigle, 2013). Other faults will be considered in future work.

A bleed valve to the atmosphere was introduced into the experimental setup after the IPT to simulate outlet leaks. Each bleed valve simulates a leak up to 3/64" in diameter. IPT Performance with various levels of outlet leaks can be seen in Figure 6.

As mentioned in the previous subsection on nominal behavior, between experiments the IPT behavior will change slightly in the "wandering set-point" phenomenon. This phenomenon also affects IPT wear behavior, and will be accounted for during modeling in Section 3, and during diagnosis in Section 4.

3. GAUSSIAN PROCESS MODELING

The experimental data used to study the performance of the current-pressure transducer is then used to train a Gaussian process data-driven model. This model predicts the outlet pressure as a function of input current, fault magnitude (outlet leak fault), and the wandering set-points. The gaussian process model is a powerful multi-dimensional interpolation technique based on spatial statistics. It is increasingly being used to build surrogates to replace expensive computer simulations in order to facilitate efficient optimization and uncertainty quantification (Rasmussen, 2004; Santner, Williams, & Notz, 2003). The GP model is preferred in this research for the following reasons: (1) it is not constrained by functional forms; (2) it is capable of representing highly nonlinear relationships in multiple dimensions; and (3) can estimate the prediction uncertainty which depends on the number and location of training data points.

The basic idea of the GP model is that the response values Y evaluated at different values of the input variables $\boldsymbol{X}$, are modeled as a Gaussian random field, with a mean and covariance function. Suppose that there are m training points, x_1, x_2, x_3 ... x_m of a d-dimensional input variable vector

($d = 4$ in this paper), yielding the output values $Y(x_1)$, $Y(x_2)$, $Y(x_3)$ ... $Y(x_m)$. The training points can be compactly written as x_T vs. y_T where the former is a $m \times d$ matrix and the latter is a $m \times 1$ vector. Suppose that it is desired to predict the response (output values y_P) corresponding to the input x_P, where x_P is $n \times d$ matrix; in other words, it is desired to predict the output at n input combinations simultaneously. Then, the joint density of the output values y_P can be calculated as:

$$p(y_P|x_P, x_T, y_T; \Theta) \sim N(m, S) \tag{1}$$

where Θ refers to the hyperparameters of the Gaussian process, which needs to be estimated based on the training data. The prediction mean and covariance matrix (m and S respectively) can be calculated as:

$$\begin{aligned} m &= K_{PT}(K_{TT} + \sigma_n^2 I)^{-1} y_T \\ S &= K_{PP} - K_{PT}(K_{TT} + \sigma_n^2 I)^{-1} K_{TP} \end{aligned} \tag{2}$$

In Eq. 2, K_{TT} is the covariance function matrix (size $m \times m$) amongst the input training points (x_T), and K_{PT} is the covariance function matrix (size $p \times m$) between the input prediction point (x_P) and the input training points (x_T). These covariance matrices are composed of squared exponential terms, where each element of the matrix is computed as:

$$K_{ij} = K(x_i, x_j; \Theta) = -\frac{\theta}{2}[\sum_{q=1}^{d} \frac{(x_{i,q} - x_{j,q})^2}{l_q}] \tag{3}$$

Note that the above computations require the estimate of the multiplicative term (θ), the length scale in all dimensions (l_q, $q = 1$ to d), and the noise standard deviation (σ_n). These constitute these hyperparameters ($\Theta = \{\theta, l_1, l_2 \ ... \ l_d, \sigma_n\}$). These hyperparameters are estimated based on the training data by maximizing the following log-likelihood function:

$$\begin{aligned} log\ p(y_T|x_T; \Theta) = &-\frac{y_T^T}{2}(K_{TT} + \sigma_n^2 I)^{-1} y_T \\ &- \frac{1}{2} log|(K_{TT} + \sigma_n^2 I)| + \frac{d}{2} log(2\pi) \end{aligned} \tag{4}$$

Once the hyperparameters are estimated, the Gaussian process model can be used for predictions using Eq. 2. Note that the "hyperparameters" of the Gaussian process are different from the "parameters" of a generic parametric model (for e.g. linear regression model). This is because, in a generic parametric model, it is possible to make predictions using only the parameters. For the Gaussian process model, all the training points and the hyperparameters are both necessary to make predictions, even though the hyperparameters may have estimated previously. For details of this method, refer to (Rasmussen, 2004; Chiles & Delfiner, 1999).

Once the training points are selected and the Gaussian process model is constructed, it can be used for diagnosis and quantifying the uncertainty in diagnosis, as explained in Section 4.

4. WEAR ESTIMATION AND UNCERTAINTY QUANTIFICATION

Wear estimation is the process of estimating the current extent of wear (i.e., quantifying the fault magnitude) on a system. This is important for prognostics (predicting failure and remaining useful life), scheduling maintenance, and triggering automated mitigation actions. This is often done using methods such as a Kalman Filter or Particle Filter (Arulampalam, Maskell, Gordon, & Clapp, 2002; Daigle, Saha, & Goebel, 2013). In this paper, recall that only steady-state measurements have been used and the transients are completely ignored. For this reason, tracking is not applicable and filtering approaches will not be suitable for wear estimation. Therefore, it is necessary to develop an algorithm that can estimate the extent of wear. Previously (Teubert & Daigle, 2013), a lookup table method was used for fault estimation. This method was chosen because of its fast, efficient nature and its ability to be applied to both linear and non-linear systems. However, this method can neither systematically account for the different sources of uncertainty nor quantifying the uncertainty in fault estimation. Hence, this paper uses the previously described Gaussian process model and Bayesian inference to quantify uncertainty in fault estimation.

As mentioned previously, this paper focuses on the outlet leak. This fault has a definite and measurable effect on the outlet pressure and can be simulated in the lab. As the leak grows in size, more gas escapes through the outlet. For a leak of 5 mm^2, the outlet pressure decreases by 2.101 psig for a high signal current and by 0.207 psig for a low signal current.

This paper focuses on quantifying the amount of wear by approaching fault estimation as a parameter estimation problem. In this technique, input-output measurements (obtained from the health monitoring sensors) are directly used to estimate the magnitude of fault; the input corresponds to the signal current (denoted by I) to the IPT, the output corresponds to the outlet pressure (denoted by P), and the magnitude of fault (wear) is denoted by θ. Further, the outlet pressure also depends on the two set-points (denoted by α_1 and α_2) that are measured during the course of health monitoring. The entire procedure for fault estimation and uncertainty quantification is described through the stepwise procedure, as shown in flowchart in Fig. 7. Each of these steps are explained in detail below.

4.1. Offline: Gaussian Process Model Development

Any parameter estimation technique relies on the existence of a forward model that can compute the quantity being measured as a function of the fault magnitude. This forward

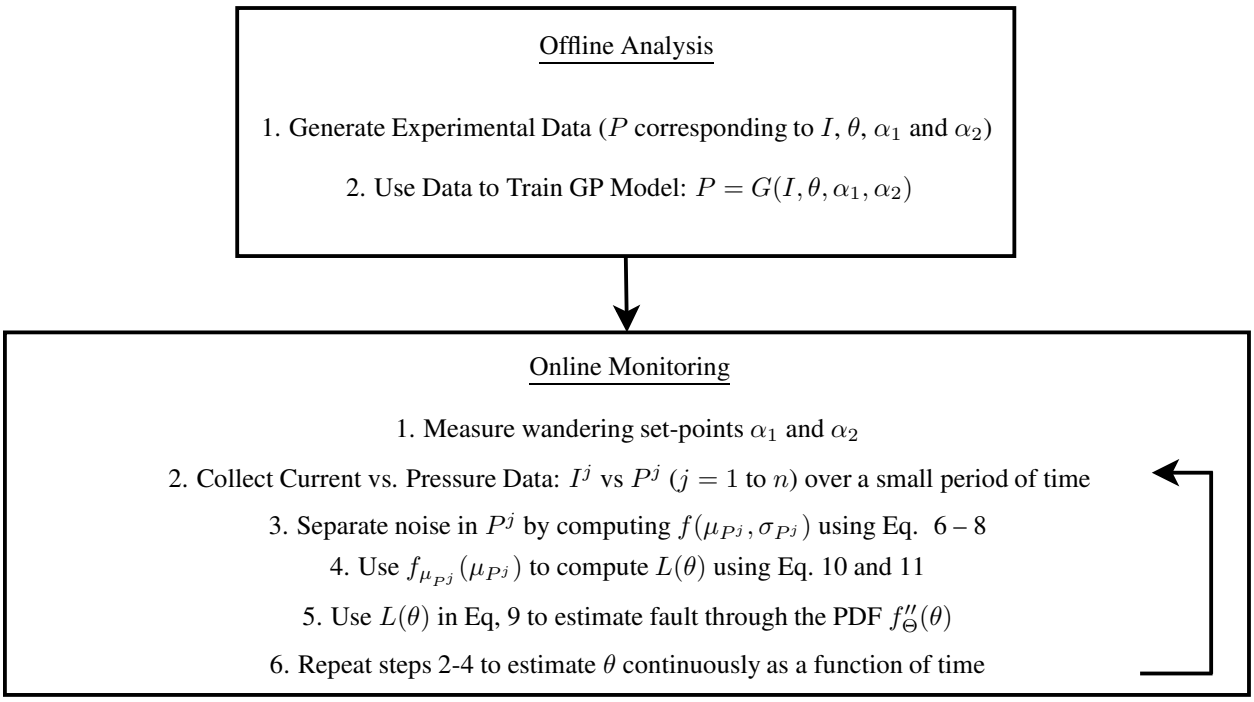

Figure 7. Stepwise Diagnosis Procedure

model is represented as:

$$P = G(I, \theta, \alpha_1, \alpha_2) \tag{5}$$

The forward model can either be physics-based or data-driven. In this paper, a fully data-driven approach is pursued. Experimental data are used to train the Gaussian process model as described in Section 3. While a rigorous design of experiments is not performed (due to the challenges involved in the experimental set up and data collection), six different runs are used to generate the training data. Each experimental run corresponds to a single pair of set-points. Within each experimental run, the fault magnitude increases gradually (as shown in Fig 15); for each value of fault magnitude, two values of I and the corresponding values of P are measured. All this data are used to train the Gaussian process model offline. After training, the model can be used for online diagnosis.

4.2. Online: Measurements and Set-Points

For performing diagnosis, the first step is to measure to set-points (α_1 and α_2); As mentioned in Section 2 IPT behavior can change over time (the "Wandering Setpoint Phenomenon"). The set-points are the outlet pressure of the undamaged system given a control input of 4 and 20 mA (the operational extremes). These values are used to quantize the wandering setpoint magnitude. Wear behavior is then dependent on the values of these set points.

Then, a small time period within which the fault magnitude is likely to be constant is considered; the current values and corresponding outlet pressure values are measured during this time period. Let I^j and P^j ($j = 1$ to n) denote the measured input-output data. The goal is to use these measurements to estimate the magnitude of fault accounting for the noise in the measurement data and other sources of uncertainty. This is accomplished through the use of the above constructed surrogate model and Bayesian inference (Sankararaman & Mahadevan, 2013). The first step is to explicitly quantify the amount of noise in the data, so that the actual steady state value may be calculated.

4.3. Separating Noise from Steady State Pressure

Consider the input-output data, described in terms of I^j versus P^j ($j = 1$ to n). In the experimental setup, the input current is treated as the independent quantity and can be controlled fully, i.e., it is assumed that there is no uncertainty regarding the current values. However, the P^j corresponds to the steady state pressure that is measured. Typically, this steady state pressure is contaminated with noise. It is important to separate out the effect of such noise. A typical steady state pressure consisting of 252 measurements is shown in Fig. 8.

One way to quantify the actual steady state value is to simply compute the average of all the measurements; however, this is not an effective treatment of uncertainty. Therefore,

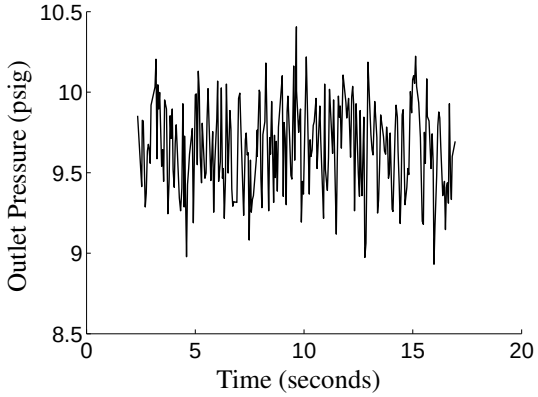

Figure 8. Steady state outlet pressure values

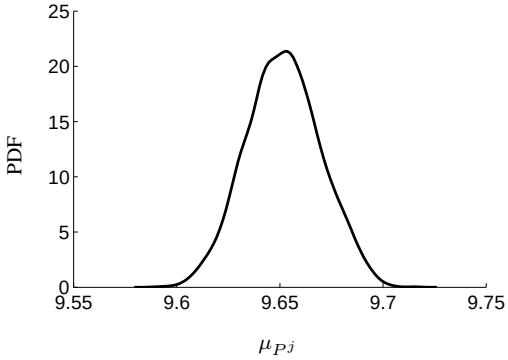

Figure 9. PDF of steady-state value (μ_{Pj})

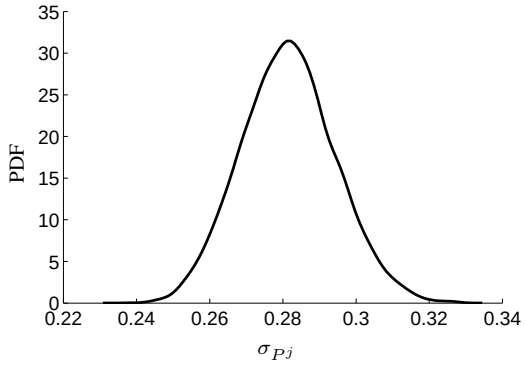

Figure 10. PDF of the standard deviation of measurement error (σ_{Pj})

this paper develops a new method to individually quantify the constant value and the noise magnitude. To this end, consider the separation of the steady state value into the constant term and noise as:

$$P^j = \mu_{Pj} + \epsilon_{Pj} \tag{6}$$

where μ_{Pj} is the actual constant steady-state value and ϵ_{Pj} is the measurement error. Further, it is assumed that the measurement error ϵ_{Pj} follows a Gaussian distribution with zero mean and standard deviation equal to σ_{Pj}. Then, based on all the measurements in Fig. 8, Bayes theorem can be used to estimate the probability distributions of both μ_{Pj} and σ_{Pj}. If the N_j (equal to 252 in Fig. 8) measurements are denoted as P_k^j ($k = 1$ to 252), then, the likelihood function $L(\mu_{Pj}, \sigma_{Pj})$ is constructed as:

$$L(\mu_{Pj}, \sigma_{Pj}) \propto \prod_{k=1}^{k=N_j} \frac{1}{\sqrt{(2\pi)}\sigma} exp\left(- \left[\frac{(\mu_{Pj} - P_k^j)^2}{\sigma_{Pj}^2} \right] \right) \tag{7}$$

Then, this likelihood function is used to estimate the joint PDF of μ_{Pj} and σ_{Pj} using Bayes theorem, as:

$$f(\mu_{Pj}, \sigma_{Pj}) = \frac{L(\mu_{Pj}, \sigma_{Pj})}{\int L(\mu_{Pj}, \sigma_{Pj}) d\mu_{Pj} d\sigma_{Pj}}. \tag{8}$$

Note that the above equation is simply a variation of Bayes' theorem; the prior distribution has been canceled in both the numerator and the denominator (inherently assuming that a constant prior has been used). It is not necessary to evaluate the above integral explicitly; instead, slice sampling (Neal, 2003) is used to directly estimate samples of μ_{Pj} and σ_{Pj} from the posterior distribution on the right hand side of the above equation. For the steady state in Fig. 8, the PDFs of μ_{Pj} and σ_{Pj} are shown in Fig. 9 and Fig. 10.

4.4. Fault Estimation through Bayesian Inference

Having the steady state, this information along with the GP model can be used to quantify the fault magnitude and the associated uncertainty. In order to achieve this goal, let $f'_\Theta(\theta)$ denote the prior probability distribution of the fault magnitude before collecting measurements; a uniform probability distribution over the entire range of possible fault magnitudes is assumed in this paper. Then, using the available input-output data, the posterior distribution of the fault magnitude (denoted by $f''_\Theta(\theta)$) is computed as:

$$f''_\Theta(\theta) = \frac{f'_\Theta(\theta) L(\theta)}{\int f''_\Theta(\theta) L(\theta) d\theta} \tag{9}$$

where $L(\theta)$ is the likelihood function of θ, defined as being proportional to the probability of observing the given input-output data conditioned on the value of the fault magnitude θ. The likelihood function, i.e., $L(\theta)$ is constructed using the estimated steady state pressure value. Recall that μ_{Pj} denotes the constant steady state pressure value and $f_{\mu_{Pj}}(\mu_{Pj})$ denotes the corresponding PDF.

Then, the likelihood function for the i^{th} input-output datapoint is expressed as:

$$L(\theta^i) \propto f_{\mu_{Pj}}(\mu_{Pj} = G(I^j, \theta, \alpha_1, \alpha_2)) \tag{10}$$

Since the n measurements are independent of one another, the combined likelihood can be calculated as:

$$L(\theta) = \prod_{i=1}^{i=n} L(\theta^i) \tag{11}$$

Then, this likelihood function is substituted into Eq. 9, and the posterior PDF of the fault magnitude θ is computed. While direct integration (Sankararaman, Ling, & Mahadevan, 2010) is used in this paper, advanced MCMC sampling methods such as slice sampling (Neal, 2003) can also be used. This procedure is repeated continuously to estimate the PDF of the fault magnitude as a function of time.

4.5. Metric for Assessing Confidence in Diagnostics

A common practice in health management is to not use the entire PDF information and simply use some central tendency of the above calculated PDF (say, mean, median, or mode) as the final diagnostic estimate. However, this procedure loses information regarding uncertainty and can lead to erroneous results. That is why it is important to quantify the confidence is diagnostic assessments. This paper discusses a simple confidence metric to address this issue.

For example, consider the mode of the PDF $f''_\Theta(\theta)$. By definition, the mode of a probability distribution has the highest likelihood of occurrence and hence is the most likely value. Therefore, the mode of the PDF $f''_\Theta(\theta)$ would be the most likely fault magnitude value. However, this implies that the true fault value may have a smaller likelihood of occurrence. Therefore, a simple way to compute a confidence metric would be to assess how far the mode (denoted by θ_C) is probabilistically away from the true estimate (denoted by θ_T). This can be computed mathematically using the likelihood ratio:

$$M = \frac{f''_\Theta(\theta_T)}{f''_\Theta(\theta_C)} \tag{12}$$

This ratio will be equal to one when the estimated mode value coincides with the true value, and in all other cases, the metric will be less than equal to one. The metric provides a probabilistic measure of confidence in the estimated fault by comparing its likelihood against the true fault magnitude. For practical purposes, the above metric can also be expressed in terms of percentage, as illustrated later in this paper.

5. NUMERICAL RESULTS

This section presents the numerical results of diagnosis uncertainty quantification on a current-pressure transducer.

5.1. Training the Gaussian Process Model

The first step is to use the experimental data to train the Gaussian process model. This model has four input quantities:

1. Fault magnitude
2. Current magnitude
3. Set-point I
4. Set-point II

For every combination of the above four quantities, the outlet steady state pressure needs to computed by the gaussian process model ($P = G(I, \theta, \alpha_1, \alpha_2)$). Hence, experimental data that depicts the variation of output pressure with respect to the four input quantities are collected and used to train the GP model. There are seven sets of data, and each set corresponds to one value of set-point I and set-point II. These experimental are shown in Figures 11—14

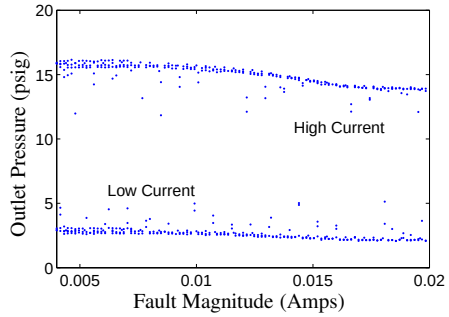

Figure 11. Fault magnitude vs. output pressure

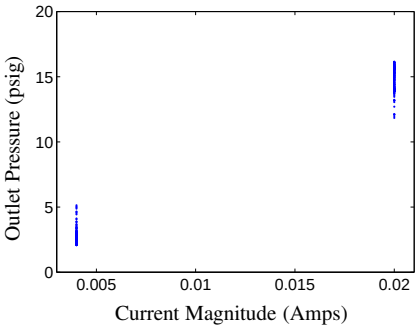

Figure 12. Current magnitude vs. output pressure

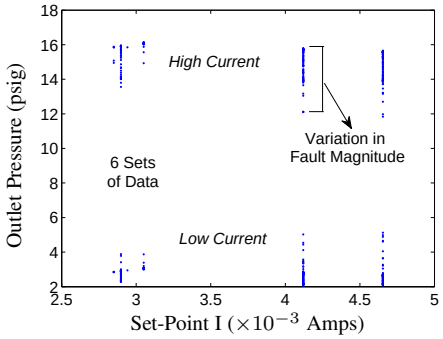

Figure 13. Set-Point I vs. output pressure

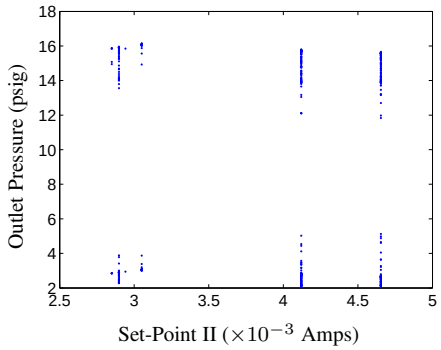

Figure 14. Set-Point II vs. output pressure

All of the above information is used to train the Gaussian process model using the procedure in Section 3. This model is used for diagnosis and quantifying the uncertainty in diagnosis.

5.2. Diagnosis: Numerical Illustration

Consider a set of current versus (steady state) outlet pressure measurements that are available through health monitoring, as shown in Fig. 15. Note that the Gaussian process model is useful for forward evaluation, i.e., to compute the outlet pressure as a function of fault magnitude and input current, and this model needs to be evaluated for multiple values of fault magnitude in order to estimate the correct fault magnitude.

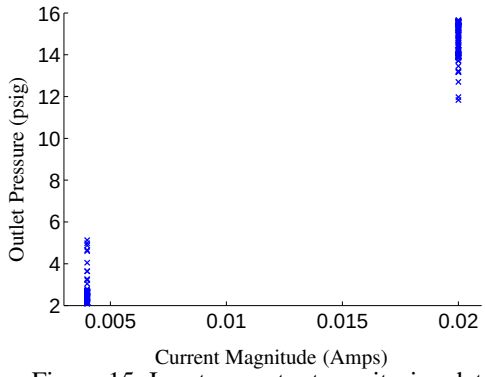

Figure 15. Input vs. output monitoring data

Two values of current are applied in an alternating manner: First, a current of 0.004 amps, and then a current of 0.02 amps. The fault magnitude is assumed to be constant over this time window. This procedure is repeated as the fault magnitude increases over time. The set-points for the above monitoring data are found to be equal to 4.65 and 15.58 milliamps. Using the Gaussian process model, and the Bayesian inference methodology explained earlier in Section 4, the fault magnitude is estimated continuously as a function of time. To estimate the fault magnitude, one low value of current and one high value of current, and the corresponding outlet pressures are considered. Since 198 sets of measurement are available and every two correspond to a single value of fault magnitude, Bayesian inference is applied 98 times to quantify the fault magnitude.

An arbitrary set of current-pressure values is chosen for the purpose of illustration; the outlet pressure values given signal currents of 0.004 amps and 0.02 amps are equal to 2.68 Pa and 15.56 Pa respectively. For these set of values, the fault magnitude is estimated using Bayesian inference; the estimated PDF and the true value are indicated in Fig. 16. Note that the mode does not correspond to the true fault magnitude.

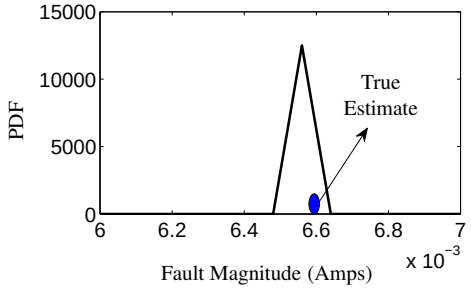

Figure 16. PDF of fault magnitude

Such computation is continuously performed with time, and the mode of the distribution is plotted against the true fault magnitude value, as shown in Fig. 17. While absolute time is not meaningful, Fig. 17 shows the number of the instance (1 through 99) in which diagnosis is performed. It can be seen that the mode approximately matches well the true fault magnitude (since the fault magnitude varies over a range, it is not possible to see succinct differences between the mode and true fault magnitudes). The methodology consistently estimates the fault magnitude and the true fault magnitude is contained within reasonable bounds of the predicted uncertainty.

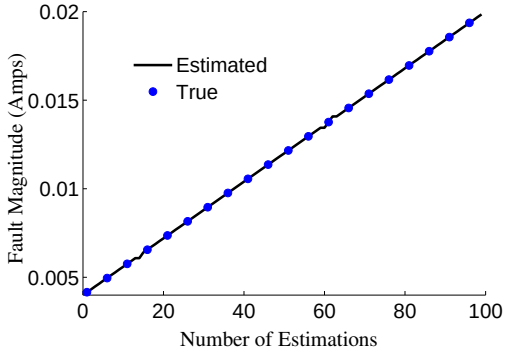

Figure 17. Fault magnitude: estimated (mode) vs. true

In addition to the mode of the fault estimate, the standard deviation is also plotted in Fig. 18, similar to Fig. 17. Note

that the standard deviation is small, as seen from Fig. 16 and Fig. 18.

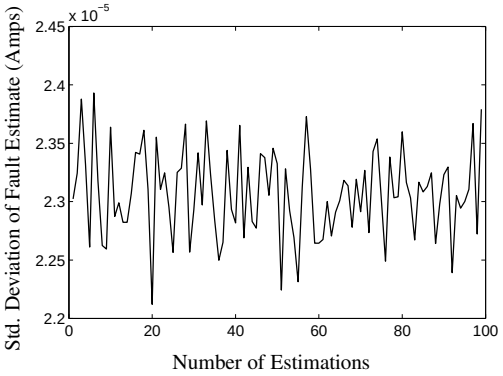

Figure 18. Uncertainty in diagnosis

However, using the proposed statistical methods, it is possible to quantify the extent of agreement between the estimated fault and true magnitude, thereby quantifying the amount of confidence in diagnosis. The metric proposed earlier in Section 4.5 (ratio of PDFs measured at the mode and the true value) is quantified and plotted (as percentage) in Fig. 19.

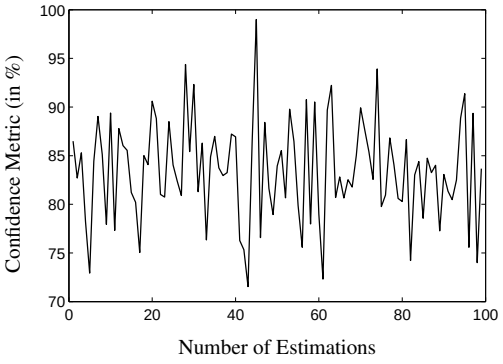

Figure 19. Confidence in diagnosis

As seen from Fig. 19, it is seen that the confidence metric is always less than 100%, suggesting that it is practically impossible to precisely estimate the true fault magnitude. A rigorous treatment of uncertainty addresses this issue by estimating the entire PDF of the fault magnitude instead of using any central tendency such as the mean, median, mode, etc.

6. CONCLUSION

This paper proposed a data-driven methodology for fault estimation and uncertainty quantification in the steady-state diagnosis of a current-pressure transducer (IPT). Such transducers are efficient electromechanical devices that can be used to control the output pressure depending on the signal current. When faults are present in these transducers, the desired pressure output may not be obtained. Therefore, it is necessary to monitor to performance of these transducers, detect the presence of faults and estimate the fault magnitude.

This is a significant challenge in diagnosis due to several sources of uncertainties associated with monitoring the heath of the transducer. To begin with, the sensors used to monitor the performance may be affected by sensor noise. Further, it may not be precisely possible to predict the performance of the transducer and this may add further uncertainty; therefore it becomes necessary to quantify the confidence in fault diagnosis.

A Bayesian inference-based methodology was used for uncertainty quantification in diagnostics, and the amount of wear (fault) was quantified as a function of time. This approach can not only systematically account for the various sources of uncertainty in the health monitoring but also quantify the uncertainty in the fault estimate, resulting in a measure of confidence in diagnosis. Experimental data were collected offline and used to develop a Gaussian process model that can predict the outlet pressure as a function of fault magnitude and input current. This Gaussian process model was then used in online diagnosis; the probability distribution of the fault magnitude and the confidence in diagnostics was estimated.

Numerical results show considerable promise of the proposed methodology. Future work may include considering multiple, simultaneous fault modes where it is necessary to quantify the uncertainty in both fault isolation and fault estimation. It is also necessary to study the effect of diagnostic uncertainty on prognosis, by quantifying the uncertainty in the remaining useful life of the transducer.

ACKNOWLEDGMENT

The study reported in this paper was partly funded by the NASA System-wide Safety Assurance Technologies (SSAT) project under the Aviation Safety (AvSafe) Program of the Aeronautics Research Mission Directorate (ARMD) and by the AGSM (Advanced Ground Systems Maintenance) project under the Ground Systems Development and Operations Program in the Human Exploration and Operations Mission Directorate. The authors also thank Dr. Chetan Kulkarni and George Gorospe at NASA Ames Research Center for their help with preparing and conducting IPT experiments on the Pneumatic Valve Testbed.

REFERENCES

Arulampalam, M. S., Maskell, S., Gordon, N., & Clapp, T. (2002). A tutorial on particle filters for online nonlinear/non-Gaussian Bayesian tracking. *IEEE Transactions on Signal Processing*, *50*(2), 174–188.

Chiles, J., & Delfiner, P. (1999). *Geostatistics: modeling spatial uncertainty* (Vol. 344). Wiley-Interscience.

Daigle, M., & Goebel, K. (2013, May). Model-based prog-

nostics with concurrent damage progression processes. *IEEE Transactions on Systems, Man, and Cybernetics: Systems*, *43*(4), 535-546.

Daigle, M., Saha, B., & Goebel, K. (2013, March). A comparison of filter-based approaches for model-based prognostics. In *Proceedings of the IEEE aerospace conference.*

Kulkarni, C., Daigle, M., & Goebel, K. (2013, sep). Implementation of prognostic methodologies to cryogenic propellant loading testbed. In *IEEE AUTOTESTCON 2013.*

Luo, J., Pattipati, K. R., Qiao, L., & Chigusa, S. (2008, September). Model-based prognostic techniques applied to a suspension system. *IEEE Transactions on Systems, Man and Cybernetics, Part A: Systems and Humans*, *38*(5), 1156 -1168.

Marsh Bellofram. (n.d.). Type 1000 i/p & e/p transducers [Computer software manual].

Neal, R. M. (2003). Slice sampling. *Annals of statistics*, 705–741.

Orchard, M., & Vachtsevanos, G. (2009, June). A particle filtering approach for on-line fault diagnosis and failure prognosis. *Transactions of the Institute of Measurement and Control*(3-4), 221-246.

Rasmussen, C. (2004). Gaussian processes in machine learning. *Advanced Lectures on Machine Learning*, 63–71.

Saha, B., & Goebel, K. (2009, September). Modeling Li-ion battery capacity depletion in a particle filtering framework. In *Proceedings of the annual conference of the prognostics and health management society.*

Sankararaman, S., Ling, Y., & Mahadevan, S. (2010). Statistical inference of equivalent initial flaw size with complicated structural geometry and multi-axial variable amplitude loading. *International Journal of Fatigue*, *32*(10), 1689–1700.

Sankararaman, S., & Mahadevan, S. (2011). Uncertainty quantification in structural damage diagnosis. *Structural Control and Health Monitoring*, *18*(8), 807–824.

Sankararaman, S., & Mahadevan, S. (2013). Bayesian methodology for diagnosis uncertainty quantification and health monitoring. *Structural Control and Health Monitoring*, *20*(1), 88–106.

Santner, T., Williams, B., & Notz, W. (2003). *The design and analysis of computer experiments*. New York: Springer-Verlag.

Teubert, C., & Daigle, M. (2013, October). I/p transducer application of model-based wear detection and estimation using steady state conditions. In *Proceedings of the annual conference of the prognostics and health management society* (p. 134-140).

Teubert, C., & Daigle, M. (2014, March). Current/pressure transducer application of model-based prognostics using steady state conditions. In *Proceedings of the IEEE aerospace conference.*

BIOGRAPHIES

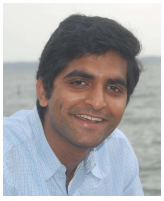

Shankar Sankararaman received his B.S. degree in Civil Engineering from the Indian Institute of Technology, Madras in India in 2007 and later, obtained his Ph.D. in Civil Engineering from Vanderbilt University, Nashville, Tennessee, U.S.A. in 2012. His research focuses on the various aspects of uncertainty quantification, integration, and management in different types of aerospace, mechanical, and civil engineering systems. His research interests include probabilistic methods, risk and reliability analysis, Bayesian networks, system health monitoring, diagnosis and prognosis, decision-making under uncertainty, treatment of epistemic uncertainty, and multidisciplinary analysis. He is a member of the American Institute of Aeronautics (AIAA), the American Society of Civil Engineers (ASCE), the Institute for Electrical and Electronics Engineers (IEEE), and the Prognostics and Health Management (PHM) Society. Currently, Shankar is a researcher at NASA Ames Research Center, where he develops algorithms for uncertainty assessment and management in the context of system health monitoring, prognostics, and decision-making.

Christopher Teubert received his B.S. in Aerospace Engineering from Iowa State University in 2012. While at Iowa State University, he conducted research on asteroid deflection mission design and asteroid fragment propagation for Iowa State Universitys Asteroid Deflection Research Center (ADRC). Previous to his current position he worked as a spacecraft systems engineer for a Mars sample return mission as part of the NASA Academy Program. He is currently developing software tools and researching algorithms for diagnostics, prognostics, and system health management for Stinger Ghaffarian Technologies, Inc. at NASA Ames Research Center in the Prognostic Center of Excellence (PCoE).

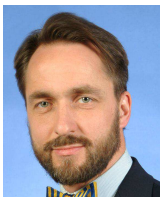

Kai Goebel is the Area Lead for Discovery and Systems Health at NASA Ames where he was director of the Prognostics Center of Excellence during the time this research was conducted. After receiving the Ph.D. from the University of California at Berkeley in 1996, Dr. Goebel worked at General Electric's Corporate Research Center in Niskayuna, NY from 1997 to 2006 as a senior research scientist before joining NASA. He has carried out applied research in the areas of artificial intelligence, soft computing, and information fusion and his interest lies in advancing these techniques for real time monitoring, diagnostics, and prognostics. He holds 17 patents and has published more than 250 papers in the area of systems health management.